Yew et al. Nanoscale Research Letters (2016) 11:276
DOI 10.1186/s11671-016-1498-2

Nanoscale Research Letters

NANO COMMENTARY Open Access

Green Synthesis of Magnetite (Fe_3O_4) Nanoparticles Using Seaweed (*Kappaphycus alvarezii*) Extract

Yen Pin Yew, Kamyar Shameli*, Mikio Miyake, Noriyuki Kuwano, Nurul Bahiyah Bt Ahmad Khairudin, Shaza Eva Bt Mohamad and Kar Xin Lee

Abstract

In this study, a simple, rapid, and eco-friendly green method was introduced to synthesize magnetite nanoparticles (Fe_3O_4-NPs) successfully. Seaweed *Kappaphycus alvarezii* (*K. alvarezii*) was employed as a green reducing and stabilizing agents. The synthesized Fe_3O_4-NPs were characterized with X-ray diffraction (XRD), ultraviolet-visible spectroscopy (UV-Vis), Fourier transform infrared (FT-IR), and transmission electron microscopy (TEM) techniques. The X-ray diffraction planes at (220), (311), (400), (422), (511), (440), and (533) were corresponding to the standard Fe_3O_4 patterns, which showed the high purity and crystallinity of Fe_3O_4-NPs had been synthesized. Based on FT-IR analysis, two characteristic absorption peaks were observed at 556 and 423 cm^{-1}, which proved the existence of Fe_3O_4 in the prepared nanoparticles. TEM image displayed the synthesized Fe_3O_4-NPs were mostly in spherical shape with an average size of 14.7 nm.

Keywords: Green synthesis, Fe_3O_4 nanoparticles, Seaweed, *Kappaphycus alvarezii*, Transmission electron microscopy

Background

With the recent rapid development and evolvement of technology, human beings have put their faith in nanotechnology and believe that it can ameliorate their current living standard [1]. As a consequence, the nanoparticle has drawn a huge interest from researchers globally due to specific characteristics such as shape, size, and distribution, which could be utilized in a distinct field of applications [2]. Synthesis of Fe_3O_4-NPs has been carried out because of its unique properties, such as being superparamagnetic [3], biocompatible, biodegradable, and expected to be non-toxic to humans [4–6]. These unique properties allow Fe_3O_4-NPs to be widely used in different areas of applications, such as catalysis [7, 8], magnetic storage media [9], biosensors [10], magnetic resonance imaging (MRI) [11, 12], and targeted drug delivery [13–15].

Numerous methods of fabrication of Fe_3O_4-NPs can be employed, such as sol-gel method [16], solid state synthesis [17], and flame spray synthesis [18]. In contrast to the time-consuming chemical and physical methods which involve complicated procedures, green method is much easier and safer to use, and plant-mediated synthesis of nanoparticles is still a new scheme and the outcome is yet to be studied. There are a couple of successful studies in synthesizing Fe_3O_4-NPs by using plant extract. For instance, fruit extract of *Artemisia annua* [19], leaf extract of *Perilla frutescens* [20], *Tridax procumbens* [21] and *caricaya papaya* [22], peel extract of plantain [23], and also seed extract of grape *proanthocyanidin* [24]. However, there are only finite studies on the synthesis of Fe_3O_4-NPs from marine plants.

Kappaphycus alvarezii (*K. alvarezii*) is a type of red seaweed from the family of *Solieriaceae*. It is well-known in the food industries for its gelling properties [25]. Carrageenan gives the thickening characteristic, which can be used as a function of green stabilizer in synthesis of nanoparticles without using hazardous chemicals. Based on the literature review, there are still no specific researches done on seaweed *K. alvarezii* for the Fe_3O_4-NPs synthesis, and this inspires and motivates

* Correspondence: kamyarshameli@gmail.com
Malaysia–Japan International Institute of Technology, Universiti Teknologi Malaysia, Jalan Sultan Yahya Petra, 54100 Kuala Lumpur, Malaysia

us to work on this. Hence, in this research, a novel green method of synthesizing Fe_3O_4-NPs using seaweed *K. alvarezii* is proposed.

Main Text

Methods

Materials

Iron (II) chloride tetrahydrate ($FeCl_2.4H_2O \geq 99$ %) and iron (III) chloride hexahydrate ($FeCl_3.\ 6H_2O$, 97 %) were purchased from Sigma-Aldrich. Sodium hydroxide (NaOH) was obtained from R&M Chemicals. All the chemicals were used without further purification. The seaweed *K. alvarezii* is a type of red seaweed which was acquired from Sabah, Malaysia. All the aqueous solutions were prepared by deionized water from ELGA Lab Water Purification System, UK. The sensION+ MM374 GLP 2 channel Benchtop Meter was employed to control the pH of the solution. An Esco Isotherm Forced Convection Laboratory Oven was used to dry the washed sample.

Preparation of Kappaphycus alvarezii Extract

The seaweed was washed under running water to remove dirt, salt, and foreign particles. Then, it was soaked overnight (24 h) in deionized water to bleach the yellowish color so that it became colorless. After that, the seaweed was rinsed and dried under sunlight for 3 days. The dried seaweed was chopped into small pieces before being blended using a hammer mill with a 3-mm filter diameter. Finally, the dried seaweed was stored until further processing. The dried seaweed reduced the storage space required and can be stored for a number of years without appreciable loss of the gelling property. In this study, 0.5 g of dried seaweed was weighed and soaked in 50 ml of deionized water for 24 h. The resulting extract was used as a seaweed extract solution.

Synthesis of K. alvarezii/Fe_3O_4-NPs

For the synthesis of *K. alvarezii*/Fe_3O_4-NPs, firstly, a solution of Fe^{3+} and Fe^{2+} with a 2:1 M ratio was added into the seaweed extract to obtain a yellowish colloidal solution. Then, the freshly prepared 1.0 M of NaOH was added drop-wise to the solution under continuous stirring. The pH of the solution was adjusted to pH 11. The solution was then stirred for 1 h to homogenize the solution and also for the completion of reaction. After that, the as-synthesized Fe_3O_4-NPs were separated by using a permanent magnet. The Fe_3O_4-NPs were washed for several times by using deionized water. The nanoparticles were dried in an oven at around 70 °C for 24 h. The dried sample was stored in an air-tight container for further characterization. All the experiments were conducted at ambient temperature.

Characterization of K. alvarezii/Fe_3O_4-NPs

The presence and phase purity of the synthesized *K. alvarezii*/Fe_3O_4-NPs were examined by using a PANalytical X'Pert PRO X-ray diffractometer (XRD). The dried sample was performed at an applied current of 20 mA and accelerating voltage of 45 kV with Cu Kα radiation ($\lambda = 1.54$ Å) at 2θ angle configuration scanning from 5° to 80° (scanning rate = 2θ/min). The UV-Vis spectrum of Fe_3O_4-NPs was determined using Shimadzu UV-Visible Spectrophotometer (UV-1800). Fourier transform infrared (FT-IR) spectroscopy was used to study the presence of the biomolecules which are responsible for the synthesis of Fe_3O_4-NPs. Dried samples were ground with potassium bromide (KBr) to produce pellet, which was examined in a wavelength range of 400–4000 cm^{-1}. The infrared absorption peaks were obtained from Thermo Scientific Nicolet 6700 Spectrometer. The size and morphology of the synthesized Fe_3O_4-NPs were observed using FEI TECNAI G2 F20 transmission electron microscope (TEM). The microscope had accelerating voltage from 20 to 200 kV and standard magnification from 22 X to 930 KX. The aqueous dispersion of the nanoparticles was dropped on 300-mesh copper grids and air-dried before viewing under a microscope. TEM images were acquired using a SC1000 ORIUS CCD Camera.

Discussion

After addition of NaOH and stirring the solution for 1 h, the color of the reaction mixture of iron chloride salts and seaweed extract changed from light brown (Fig. 1a) to black (Fig. 1b), which indicates the formation of Fe_3O_4-NPs. Separation of Fe_3O_4-NPs could be done with the aid of an external permanent magnet. Figure 1c clearly reveals that the synthesized Fe_3O_4-NPs is able to be attracted by an external permanent magnet quickly, which proved that the nanoparticles possessed magnetic properties. Once the magnet was removed, the nanoparticles were dispersed readily by shaking.

Fe_3O_4 nanoparticles are prepared by adding a base to an aqueous mixture of Fe^{3+} and Fe^{2+} chloride at a 2:1 M ratio. The chemical reaction of Fe_3O_4 precipitation is given in Eqs. 1 and 2. The overall reaction may be written as follows:

$$K.\ alvarezii + H_2O_{(l)} + Fe^{2+}_{(aq)} + Fe^{3+}_{(aq)} \xrightarrow{Stirring} [K.\ alvarezii/Fe^{3+}\text{-}Fe^{2+}] \quad (1)$$

$$[K.\ alvarezii/Fe^{3+}\text{-}Fe^{2+}] + 80H^-_{(aq)} \xrightarrow{Stirring} [K.\ alvarezii/Fe_3O_4]\downarrow_{(s)} + 4H_2O_{(aq)} \quad (2)$$

The precipitation occurs because of the Fe_3O_4-NPs have a high tendency to aggregate into agglomerates as

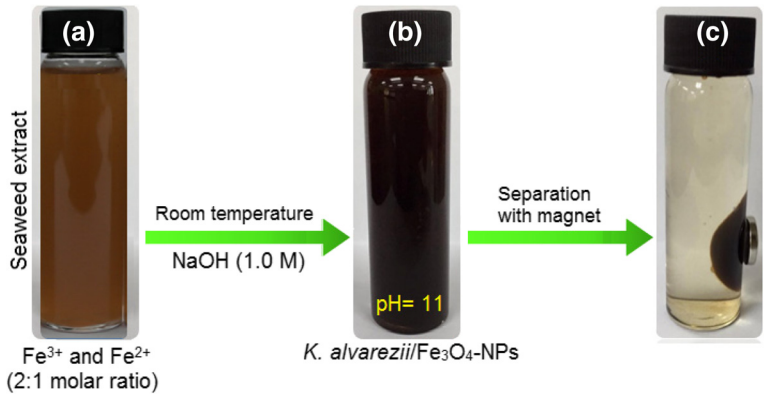

Fig. 1 **a** Solution of Fe^{3+} and Fe^{2+} with 2:1 M ratio and seaweed *K. alvarezii* extract. **b** *K. alvarezii*/Fe_3O_4-NPs. **c** Separation of synthesized Fe_3O_4-NPs from reaction mixture using an external magnet

to decrease the energy associated with the large surface area to volume ratio, a phenomenon which is likely deteriorated by the low surface charge [26].

UV-Vis Spectral Analysis

The UV-Vis spectroscopy of seaweed *K. alvarezii* and synthesized Fe_3O_4-NPs are shown in Fig. 2. Seaweed *K. alvarezii* does not show any absorption peak (blue). However, the synthesized Fe_3O_4-NPs reveals continuous absorption in the visible range of 300–800 nm without any strong absorption peak (red). Studies from Basavegowda et al. had reported identical UV-Vis spectra for Fe_3O_4-NPs synthesized using *A. annua* and *P. frutescens* extracts [19, 20].

XRD Analysis

Phase purity and crystallinity of the synthesized Fe_3O_4-NPs can be identified via XRD analysis. The XRD patterns of seaweed *K. alvarezii* and synthesized Fe_3O_4-NPs are shown in Fig. 3. A broad diffraction peak was observed (Fig. 3a) at 21.50°, which is attributed to seaweed *K. alvarezii*. This is confirmed by a study which showed unanimous XRD patterns of seaweed *K. alvarezii* that were used in the synthesis of $Cu@Cu_2O$ core shell nanoparticles [27]. The diffraction peaks of synthesized Fe_3O_4-NPs (Fig. 3b) were detected at $2\theta = 30.56°$, 35.86°, 43.46°, 54.01°, 57.38°, 63.00°, and 74.46°, which are assigned to the crystal planes of (200), (311), (400), (422), (511), (440), and (533), respectively. The analyzed diffraction peaks were matched well with the standard magnetite XRD patterns with JCPDS file no: 00-003-0863, which declared the crystallographic system of cubic structure. Besides, the synthesized nanoparticles were affirmed to be Fe_3O_4 but not maghemite (γ-Fe_2O_3) by comparing the XRD patterns with the standard

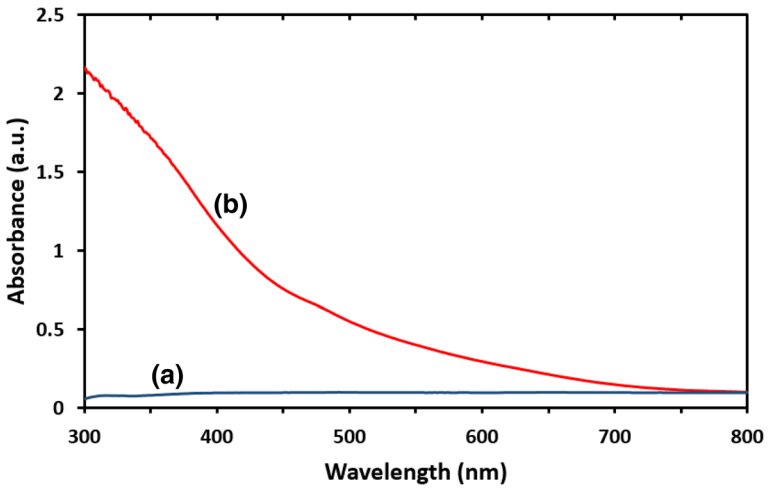

Fig. 2 UV-vis absorption spectra of (***a***) seaweed *K. alvarezii*. (***b***) Synthesized Fe_3O_4-NPs

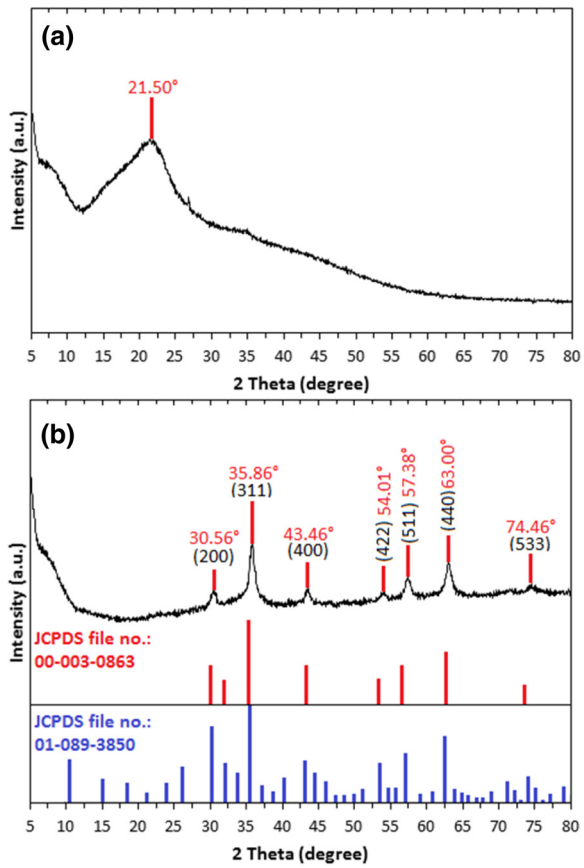

Fig. 3 XRD patterns of **a** seaweed *K. alvarezii*. **b** Synthesized Fe_3O_4-NPs

maghemite JCPDS file no.: 01-089-3850. A huge difference can be clearly seen in that the XRD patterns of γ-Fe_2O_3 consist of many peaks, unlike Fe_3O_4 which only involves few peaks. Estimation of the crystallite size of synthesized Fe_3O_4-NPs can be calculated by using the Debye-Scherrer equation [28], which reveals a relationship between X-ray diffraction peak broadening and crystallite size. The Debye-Scherrer equation is shown as follows:

$$d = \frac{k\lambda}{\beta_{hkl} cos\theta_{hkl}},$$

where d is the crystallite size of synthesized Fe_3O_4-NPs for (hkl) phase, k is Scherrer constant (0.9), λ is the X-ray wavelength of radiation for Cu Kα (0.154 nm), β_{hkl} is the full-width at half maximum (FWHM) at (hkl) peak in radian, and θ_{hkl} is the diffraction angle for (hkl) phase. Using the equation, the estimated crystallite size of synthesized Fe_3O_4-NPs was 16.79 nm, which was calculated from the full-width at half maximum of the Fe_3O_4 (311) diffraction peak [29] at $2\theta = 35.86°$. Based on the X-ray diffraction pattern, the synthesized Fe_3O_4-NPs were figured out to be high purity crystalline, as no impurity peak was observed.

Transmission Electron Microscopy Study

The size and morphology of the synthesized Fe_3O_4-NPs were analyzed by using TEM. The TEM image of synthesized Fe_3O_4-NPs (Fig. 4a) showed that majority of the nanoparticles were in spherical shape. The image revealed that most of the particles were agglomerated, which might be due to the thickening properties of seaweed *K. alvarezii* or the presence of hydroxyl groups from the extract [30]. Besides, the tendency of agglomeration is not surprising as the synthesized Fe_3O_4-NPs is small in size and possess magnetic characteristics [31]. A histogram of particle size distribution was drawn according to the size of 70 nanoparticles (Fig. 4b). The mean particle size was 14.7 nm with the standard deviation of 1.8 nm. The crystallite size of the synthesized Fe_3O_4-NPs was found to be 16.7 nm from XRD analysis, which is in an agreement with the result obtained from the TEM

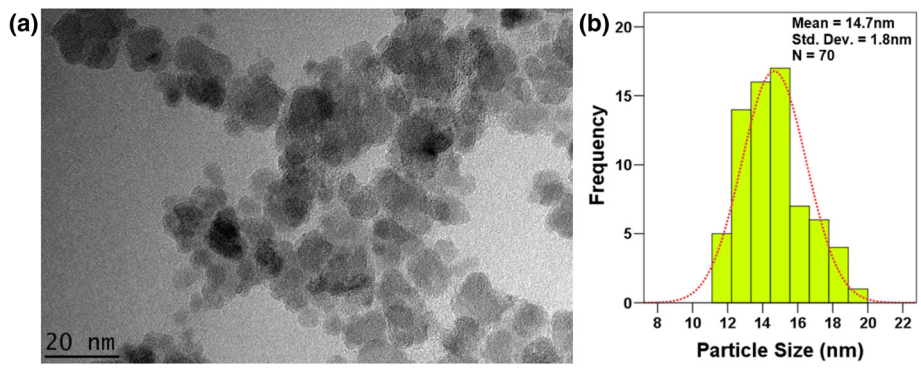

Fig. 4 **a** TEM image of the synthesized Fe_3O_4-NPs at magnification of 35 KX. **b** Size distribution histogram of the synthesized Fe_3O_4-NPs

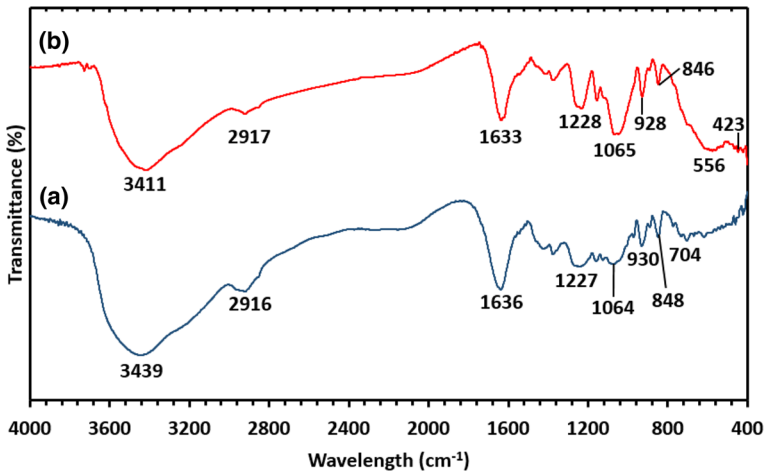

Fig. 5 FT-IR spectra of (***a***) seaweed *K. alvarezii*. (***b***) Synthesized Fe_3O_4-NPs

that shows a size distribution between 11.0 and 20.0 nm. A few very small spherical objects can be observed from the image which might be due to the residue of seaweed *K. alvarezii.*

Fourier Transform Infrared Study

FT-IR spectroscopy was performed to determine the functional groups of seaweed *K. alvarezii* that acted as a stabilizer and capping agent in the synthesis of Fe_3O_4–NPs. The spectra of the seaweed *K. alvarezii* extract revealed strong absorption bands at 3439, 2916, 1636, 1227, 1064, 930, 848, and 704 cm^{-1} (Fig. 5a), while the absorption bands of synthesized Fe_3O_4-NPs were observed at 3411, 2917, 1633, 1228, 1065, 928, 846, 556, and 423 cm^{-1} (Fig. 5b). The absorption peak of 3439 cm^{-1} in the *K. alvarezii* extract indicated the O–H stretching vibration. The absorption peaks at 2916 cm^{-1} contributed to the C–H stretching vibrations of the $-CH_2$ functional group [32], while 1636 cm^{-1} were attributed to the C–H bending overtone band of aromatic compound. Absorption peak at 1227 cm^{-1} corresponded to the asymmetric stretching vibration of the sulfate group [33], whereas peak at 1064 cm^{-1} was assigned to the C–O stretching band related to the C–O–SO_3 group [34]. The absorption peaks 930, 848, and 704 cm^{-1} revealed the existence of aromatic C–H bending band. All the bands were shifted, indicating the participation and interaction of nanoparticles with the seaweed *K. alvarezii* extract [35, 36]. Two significant new peaks were found at 556 and 423 cm^{-1} in the spectra of synthesized Fe_3O_4-NPs, which is associated with the stretching vibration mode of Fe–O. The metal-oxygen band at 556 cm^{-1} corresponded to intrinsic stretching vibrations of metal at the tetrahedral site, while the metal-oxygen band found at 423 cm^{-1} was assigned to octahedral-metal stretching of Fe–O [37].

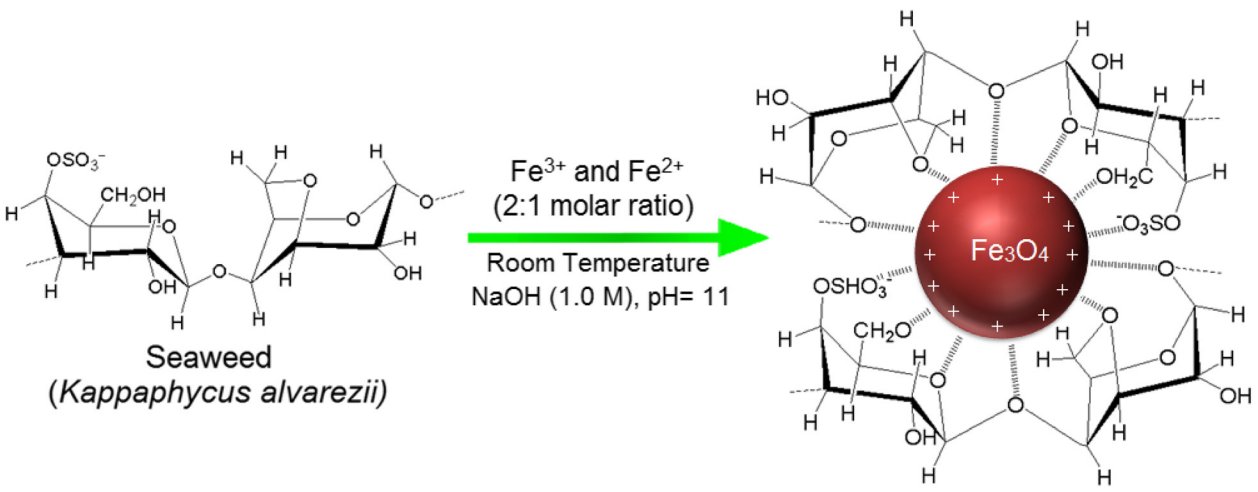

Fig. 6 Schematic diagram demostrating the interaction between Fe_3O_4-NPs-charged groups which are capped by seaweed *K. alvarezii*

The formation of Fe_3O_4-NPs was confirmed with these characteristic peaks as the peaks laying in the region between 400 and 600 cm^{-1} were corresponding to Fe_3O_4 [28].

A presumed schematic diagram of formation of *K. alvarezii*/Fe_3O_4-NPs is illustrated in Fig. 6, where the presence of van der Waals forces holds the positively charged Fe_3O_4-NPs and negatively charged groups presenting in the molecular structure of seaweed *K. alvarezii* together [38].

Conclusions

In this study, Fe_3O_4-NPs were synthesized successfully by a simple and green approach using the seaweed *K. alvarezii* extract without utilizing any chemical-reducing agent and stabilizer. Based on the XRD analysis studied, a high purity crystalline of Fe_3O_4-NPs was prepared. FT-IR spectroscopy showed the involvement biomolecules present in the extract of seaweed *K. alvarezii*, which were verified in the synthesizing process of Fe_3O_4-NPs. The formation of Fe_3O_4-NPs was confirmed due to the noticeable absorption peaks at 556 and 423 cm^{-1}. TEM result revealed the size and morphology of the synthesized Fe_3O_4-NPs. Most of the particles possessed spherical shapes with average particle sizes of 14.7 nm. The non-toxic green synthesized Fe_3O_4-NPs are expected suitable to be employed in various fields of applications, especially in biomedical applications.

Abbreviations

NPs nanoparticles, *K. alvarezii Kappaphycus alvarezii*, *XRD* X-ray diffraction, *UV-Vis* ultraviolet-visible spectroscopy, *FT-IR* Fourier transform infrared, TEM transmission electron microscopy

Competing Interests

The authors declare that they have no competing interests.

Authors' Contributions

YPY and KS carried out the synthesis and characterization of the compounds. YPY, KS, MM, NK, NBBAK, SEBM, and KXL carried out the acquisition of data, analysis and interpretation of the data collected, were involved in the drafting of the manuscript and revision of the draft for important intellectual content, and gave final approval of the version to be published. All authors read and approved the final manuscript.

Acknowledgements

This research was supported by the grant funded by the Ministry of education (Reference grant number PY/2015/05547 under FRGS grant). Also, the authors would like to express their gratitude to the Research Management Centre (RMC) of UTM for providing a conducive environment to carry out this research.

Received: 4 February 2016 Accepted: 23 May 2016
Published online: 02 June 2016

References

1. Priest S (2006) The North American opinion climate for nanotechnology and its products: opportunities and challenges. J Nanopart Res 8(5):563–568
2. Zargar M, Hamid AA, Bakar FA, Shamsudin MN, Shameli K, Jahanshiri F, Farahani F (2011) Green synthesis and antibacterial effect of silver nanoparticles using *Vitex negundo* L. Molecules 16(8):6667–6676
3. Mahdavian AR, Mirrahimi MAS (2010) Efficient separation of heavy metal cations by anchoring polyacrylic acid on superparamagnetic magnetite nanoparticles through surface modification. Chem Eng J 159(1):264–271
4. Hu FQ, Wei L, Zhou Z, Ran YL, Li Z, Gao MY (2006) Preparation of biocompatible magnetite nanocrystals for in vivo magnetic resonance detection of cancer. Adv Mater 18(19):2553–2556
5. Zhao H, Saatchi K, Häfeli UO (2009) Preparation of biodegradable magnetic microspheres with poly(lactic acid)-coated magnetite. J Magn Magn Mater 321(10):1356–1363
6. Zhang L, Dong WF, Sun HB (2013) Multifunctional superparamagnetic iron oxide nanoparticles: design, synthesis and biomedical photonic applications. Nanoscale 5(17):7664–7684
7. GawandeMB BPS, Varma RS (2013) Nano-magnetite (Fe3O4) as a support for recyclable catalysts in the development of sustainable methodologies. Chem Soc Rev 42(8):3371–3393
8. Sharad NS, Swapnil RB, Ganesh RM, Samadhan SK, Dinesh KM, Shashikant BB, Anuj KR, Nenad B, Orlando MNDT, Radek Z, Rajender SV, Manoj BG (2014) Iron oxide-supported copper oxide nanoparticles (nanocat-Fe-CuO): magnetically recyclable catalysts for the synthesis of pyrazole derivatives, 4-methoxyaniline, and ullmann-type condensation reactions. ACS Sustainable Chem Eng 2(7):1699–1706
9. Terris BD, Thomson T (2005) Nanofabricated and self-assembled magnetic structures as data storage media. J Phys D Appl Phys 38(12):R199–R222
10. Kavitha AL, Prabu HG, Babu SA, Suja SK (2013) Magnetite nanoparticles-chitosan composite containing carbon paste electrode for glucose biosensor application. J Nanosci Nanotechnol 13(1):98–104
11. Haw CY, Mohamed F, Chia CH, Radiman S, Zakaria S, Huang NM, Lim HN (2010) Hydrothermal synthesis of magnetite nanoparticles as MRI contrast agents. Ceram Int 36(4):1417–1422
12. Qiao RR, Yang CH, Gao MY (2009) Superparamagnetic iron oxide nanoparticles: from preparations to in vivo MRI applications. J Mater Chem 19(35):6274–6293
13. Salem M, Xia Y, Allan A, Rohani S, Gillies ER (2015) Curcumin-loaded, folic acid-functionalized magnetite particles for targeted drug delivery. RSC Adv 5(47):37521–37366
14. Li XL, Li H, Liu GQ, Deng ZW, Wu SL, Li PH, Xu ZS, Xu HB, Chu PK (2012) Magnetite-loaded fluorine-containing polymeric micelles for magnetic resonance imaging and drug delivery. Biomaterials 33(10):3013–3025
15. Wani KD, Kadu BS, Mansara P, Gupta P, Deore AV, Chikate RC, Poddar P, Dhole SD, Kaul-Ghanekar R (2014) Synthesis, characterization and in vitro study of biocompatible cinnamaldehyde functionalized magnetite nanoparticles (CPGF Nps) for hyperthermia and drug delivery applications in breast cancer. Plos One 9(9):e107315. doi:10.1371/journal.pone.0107315
16. Lemine OM, Omri K, Zhang B, El Mir L, Sajieddine M, Alyamani A, Bououdina M (2012) Sol–gel synthesis of 8 nm magnetite (Fe_3O_4) nanoparticles and their magnetic properties. Superlattice Microst 52(4):793–799
17. Paiva DL, Andrade AL, Pereira MC, Fabris JD, Domingues RZ, Alvarenga ME (2015) Novel protocol for the solid-state synthesis of magnetite for medical practices. Hyperfine Interact 232:19–27
18. Kumfer BM, Shinoda K, Jeyadevan B, Kennedy IM (2010) Gas-phase flame synthesis and properties of magnetic iron oxide nanoparticles with reduced oxidation state. J Aerosol Sci 41(3):257–265
19. Basavegowda N, Magar KBS, Mishra K, Lee YR (2014) Green fabrication of ferromagnetic Fe_3O_4 nanoparticles and their novel catalytic applications for the synthesis of biologically interesting benzoxazinone and benzthioxazinone derivatives. New J Chem 38(11):5415–5420
20. Basavegowda N, Mishra K, Lee YR (2014) Sonochemically synthesized ferromagnetic Fe_3O_4 nanoparticles as a recyclable catalyst for the preparation of pyrrolo [3, 4-*c*] quinoline-1,3-dione derivatives. RSC Adv 4(106):61660–61666
21. Senthil M, Ramesh C (2012) Biogenic synthesis of Fe_3O_4 nanoparticles using *Tridax procumbens* leaf extract and its antibacterial activity on pseudomonas aeruginosa. Dig J Nanomater Biostruct 7(4):1655–1659
22. Latha N, Gowri M (2014) Biosynthesis and characterisation of Fe_3O_4 nanoparticles using *Caricaya papaya* leaves extract. Int J Sci Res 3(11):1551–1556
23. Venkateswarlu S, Rao YS, Balaji T, Prathima B, Jyothi NVV (2013) Biogenic synthesis of Fe_3O_4 magnetic nanoparticles using plantain peel extract. Mater Lett 100:241–244
24. Narayanan S, Sathy BN, Mony U, Koyakutty M, Nair SV, Menon D (2012) Biocompatible magnetite/gold nanohybrid contrast agents via green chemistry for MRI and CT bioimaging. ACS Appl Mater Interfaces 4(1):251–260

25. Raman M, Doble M (2014) Physicochemical and structural characterisation of marine algae *Kappaphycus alvarezii* and the ability of its dietary fibres to bind mutagenic amines. J Appl Phycol 26(5):2183–2191
26. Valentin VM, Svetlana SM, Andrew JL, Olga VS, Anna OD, Igor VY, Michael ET, Natalia OK (2014) Biosynthesis of stable iron oxide nanoparticles in aqueous extracts of *Hordeum vulgare* and *Rumex acetosa* plants. Langmuir 30(20):5982–5988
27. Khanehzaei H, Ahmad MB, Shameli K, Ajdari Z (2014) Synthesis and characterization of Cu@Cu_2O core shell nanoparticles prepared in seaweed *Kappaphycus alvarezii* media. Int J Electrochem Sci 9:8189–8198
28. Yuvakkumar R, Hong SI (2014) Green synthesis of spinel magnetite iron oxide nanoparticles. Adv Mater Res 1051:39–42
29. Sofia S, Gawande MB, Alexandre V, João PV, Nenad B, João T, Alexander T, Orlando MNDT, Radek Z, Rajender SV, Paula SB (2014) Magnetically recyclable magnetite-palladium (Nanocat-Fe-Pd) nanocatalyst for the Buchwald-Hartwig reaction. Green Chem 16(7):3494–3500
30. Venkateswarlu S, Yoon MY (2015) Surfactant-free green synthesis of Fe_3O_4 nanoparticles capped with 3, 4-dihydroxyphenethylcarbamodithioate: stable recyclable magnetic nanoparticles for the rapid and efficient removal of Hg(II) ions from water. J Chem Soc Dalton Trans 44(42):18427–18437
31. Manoj BG, Anuj KR, Isabel DN, Rajender SV, Paula SB (2013) Magnetite-supported sulfonic acid: a retrievable nanocatalyst for the Ritter reaction and multicomponent reactions. Green Chem 15(7):1895–1899
32. Awwad AM, Salem NM (2012) A green and facile approach for synthesis of magnetite nanoparticles. J Nanosci Nanotechnol 2(6):208–213
33. Mahdavi M, Namvar F, Ahmad MB, Mohamad R (2013) Green biosynthesis and characterization of magnetic iron oxide (Fe_3O_4) nanoparticles using seaweed (*Sargassum muticum*) aqueous extract. Molecules 18(5):5954–5964
34. Camara FBG, Costa LA, Fidelis GP, Nobre LTDB, Dantas-Santos N, Cordeiro SL, Costa MSSP, Alves LG, Rocha HAO (2011) Heterofucans from the brown seaweed *Canistrocarpus cervicornis* with anticoagulant and antioxidant activities. Ma Drugs 9(1):124–138
35. Venkateswarlu S, Kumar BN, Prasad CH, Venkateswarlu P, Jyothi NVV (2014) Bio-inspired green synthesis of Fe_3O_4 spherical magnetic nanoparticles using *Syzygium cumini* seed extract. Physica B Condens Matter 449:67–71
36. Abdullah NIS, Ahmad MB, Shameli K (2015) Biosynthesis of silver nanoparticles using *Artocarpus elasticus* stem bark extract. Chem Cent J 9(1):1–7
37. Demir A, Topkaya R, Baykal A (2013) Green synthesis of superparamagnetic Fe_3O_4 nanoparticles with maltose: its magnetic investigation. Polyhedron 65:282–287
38. Elsupikhe RF, Shameli K, Ahmad MB, Ibrahim NA, Zainudin N (2015) Green sonochemical synthesis of silver nanoparticles at varying concentrations of k-carrageenan. Nanoscale Res Lett 10(1):302. doi:10.1186/s11671-015-0916-1